The Journal of Experimental Biology 207, 461-474
Published by The Company of Biologists 2004
doi:10.1242/jeb.00769

Kinematics of the transition between aquatic and terrestrial locomotion in the newt *Taricha torosa*

Miriam A. Ashley-Ross* and Brett F. Bechtel
Department of Biology, Box 7325, Wake Forest University, Winston-Salem, NC 27109, USA
*Author for correspondence (e-mail: rossma@wfu.edu)

Accepted 27 October 2003

Summary

California newts *(Taricha torosa)* are capable of locomotion in both aquatic and terrestrial environments. The transition between swimming and terrestrial walking was examined by videotaping individual *Taricha* walking both up and down a ramp, inclined at 15° to the horizontal, that had its lower end immersed in water and its upper end out of the water. When ascending the ramp, California newts first approached it by swimming, then used their limbs to walk while still in water, and finally left the water using a normal terrestrial walking gait. The reverse of this sequence was observed when individuals descended the ramp. In both directions, *Taricha* used a lateral sequence walk with a duty factor of approximately 76% when out of the water. Timing of footfalls was more variable in water and featured shorter duty factors, leading to periods of suspension. Comparison of angular and timing variables revealed effects due to direction and degree of immersion. Few timing variables showed differences according to stride within sequence (indicating whether the animal was in or out of the water), suggesting that the basic walking pattern is equally good in both environments.

Key words: newt, salamander, *Taricha torosa*, kinematics, terrestrial locomotion, aquatic locomotion.

Introduction

The view of tetrapod evolution typically presented in undergraduate textbooks is that limbs evolved specifically for terrestrial locomotion, which was of selective advantage in a Devonian environment subject to drought (e.g. Campbell et al., 1999; Pough et al., 2002). Sarcopterygian fishes are pictured as moving from stream to stream, or pond to pond, using their lobed fins as flexible props; these fins eventually gave rise to full-fledged tetrapod limbs (Campbell et al., 1999). The lobed fins were thought to be, in essence, preadapted for later function as terrestrial limbs; the movement pattern of the paired fins in the coelacanth strongly resembles a tetrapod trot, although *Latimeria* uses its fins for aquatic propulsion (Fricke et al., 1987).

However, in the past 15 years, evidence has emerged that challenges this view. Edwards (1989) points out that bottom-dwelling antennariid anglerfishes use their paired pectoral and pelvic fins to traverse the substrate in a manner analogous to limbs. The fins of these animals are fleshy and outwardly resemble limbs. Antennariids even switch between two recognizable tetrapod gaits: the lateral sequence walk and the transverse gallop (albeit at extremely low speeds; Edwards, 1989). Although the antennariids are fully aquatic and not closely related to the evolutionary line that gave rise to tetrapods, the submerged gaits are nonetheless demonstrative of the usefulness of limbs (or limb-like structures) for certain types of underwater locomotion.

More compelling to a re-thinking of the evolution of the tetrapod limb is evidence from recent fossil finds, indicating that the appearance of limbs pre-dates the move onto land (Clack, 2002a,b). For instance, *Acanthostega*, one of the earliest described tetrapods from the Upper Devonian, has been reconstructed as possessing fully developed tetrapod limbs but also equipped with fish-like internal gills in an opercular chamber (Coates and Clack, 1991). The later-occurring *Pederpes* (Early Carboniferous) retains evidence of a lateral line system in the skull, suggesting aquatic activity, while also possessing limbs resembling those of late Carboniferous forms thought to be primarily terrestrial (Clack, 2002a,b).

Previous studies of limbed locomotion in vertebrates have examined primarily terrestrial movements (e.g. Hildebrand, 1985) and discussed adaptations of particular groups to different modes of locomotion (e.g. cursorial *versus* fossorial animals). However, if tetrapod limb structure indeed evolved in an aquatic environment, then the original function of the tetrapod limb was to facilitate underwater, not terrestrial, locomotion. While we have an excellent understanding of aquatic locomotion *via* axial propulsion (e.g. Gillis, 1997, 1998b; Hammond et al., 1998; Jayne and Lauder, 1994, 1995; Long et al., 1996), studies of limb use during aquatic locomotion are few. The existing studies on limb use in water have examined turtles (Pace et al., 2001), toads (Gillis and Biewener, 2000) and ducks (Biewener and Corning, 2001); all

of these taxa depart significantly from the plesiomorphic tetrapod body plan. The study of the function of tetrapod limbs in providing aquatic propulsion is thus of fundamental importance in enhancing our understanding of the evolution of a major mode of vertebrate locomotion.

While it would be ideal to examine underwater locomotion in primitive tetrapods, no such species are available to us. Among extant vertebrate groups, the closest analog to the movement pattern of the earliest tetrapods is found in the salamanders (Edwards, 1989). Salamanders resemble early tetrapods in general body form, and salamander morphology has remained essentially unchanged for at least 150 million years (Gao and Shubin, 2001). Workers in the field of neural circuit modeling have used salamanders as a surrogate for primitive tetrapods in their endeavors to model the control of locomotor movements (Ijspeert, 2000, 2001). Indeed, Ijspeert (2001) has shown that movements matching the traveling axial waves of swimming and the standing waves of trotting can be produced by a simple neuronal circuit in the salamander model and that the switch between these gaits in the model can likewise be generated by minor changes in the circuit.

Many adult salamanders spend a large proportion of their lives near or in water (Duellman and Trueb, 1986), and thus their limbs must be able to carry out both aquatic and terrestrial locomotion effectively. Previous research on salamander locomotion has tended to focus almost exclusively on terrestrial locomotion (e.g. Ashley-Ross, 1994a,b, 1995; Barclay, 1946; Daan and Belterman, 1968; Edwards, 1977). Aquatic locomotion in salamanders has been studied only in reference to the axial musculoskeletal system (Frolich and Biewener, 1992; Gillis, 1997). Few studies have explicitly dealt with how the same locomotor structures are used in different environments (Carrier, 1993; Ellerby et al., 2001; Gillis 1998a, 2000; Gillis and Blob, 2001) or how larval and adult structures function in the same (terrestrial) environment (Ashley-Ross, 1994b).

In the present study, we quantify the kinematics of the transition between terrestrial walking and aquatic locomotion (submerged walking and/or swimming). We demonstrate that limb and body movement patterns differ with successive strides during the transition and that kinematics differ according to the direction of the transition.

Materials and methods

Animals

The California newt (*Taricha torosa* Rathke 1833) has an aquatic larval stage followed by metamorphosis into a terrestrial juvenile that is visually indistinguishable from the sexually mature adult stage. Unlike European newts, *Taricha* never develops a median dorsal crest, even when reproductive adults return to the water to breed. With the exception of reproductive activity, adult *Taricha* live primarily on land, beneath cover or underground (Petranka, 1998). Four metamorphosed individuals were purchased from local pet suppliers, brought into the lab and maintained in a common 40 liter terrarium with *ad libitum* access to water. They were fed 2–3 times per week on a diet of waxworms and small crickets. Snout–vent lengths (*SVL*) of animals ranged from 5.95 cm to 6.52 cm at the time of the experiments. All trials were performed at room temperature (~25°C).

Video recording

Newts were videotaped walking both up and down an acrylic ramp, positioned with its lower half submerged in water (Fig. 1). The ramp was set at an angle of 15° to the horizontal by supporting one end with a solid block. The surface of the ramp was covered by adhesive plastic panels with a rough texture, to provide secure footing for the newts, and marked with a series of dots spaced 1 cm apart. A vertical 1 cm grid was also placed next to the ramp to allow calibration of lateral images.

Two JVC GR-DVL9800 digital camcorders, one placed above the tank to afford a dorsal view and one placed in front of the tank to capture a lateral view, were tilted so that they were aligned perpendicular to the ramp surface and ramp long axis, respectively. Both cameras captured images at a rate of 60 fields s^{-1}. Video records from the two cameras were synchronized by a discrete event visible in both the dorsal and lateral views.

Video analysis

Only sequences in which the newt showed continuous, steady-speed motion were selected for analysis. Sequences where the animal paused or stopped between successive strides were not used. Five sequences in each direction (ramp-to-water and water-to-ramp) were obtained from each animal. Video recordings were captured using Adobe Premiere 6.5 (Adobe Systems, Inc., San Jose, CA, USA) into a Macintosh computer.

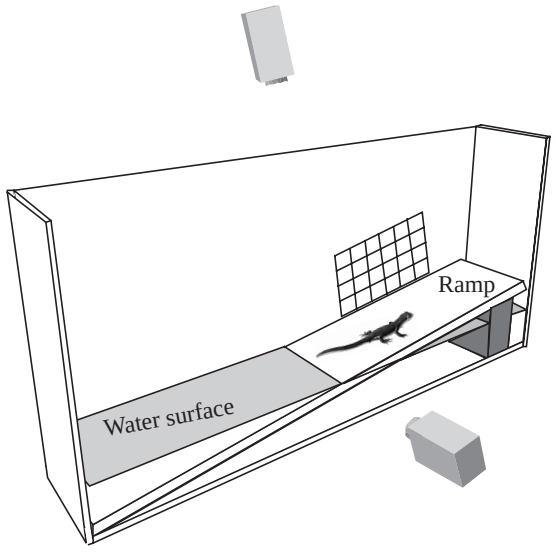

Fig. 1. Schematic of the experimental setup for videotaping sequences. The chamber is a 40-liter aquarium partially filled with water. For clarity, the front wall of the aquarium has been omitted from the illustration.

Video files were exported as sequences of TIFF files. DeBabelizer Pro 5 (Equilibrium Technologies, San Rafael, CA, USA) was used to de-interlace the two fields of each frame and convert the images to JPEG format. The custom video analysis program Didge (written by Alistair Cullum of Creighton University and available for download at http://biology.creighton.edu/faculty/cullum/Didge/) was used to determine the (*x*, *y*) coordinates for anatomical landmarks (see below). Sequences of images from the dorsal and lateral views were digitized independently. From both views, the following points were digitized: the tip of the snout, the vertebral column midway between the shoulder joints, the vertebral column midway between the limb girdles, the vertebral column midway between the hip joints, and the limbs nearest the front tank wall: the shoulder, elbow, wrist, hip, knee and ankle joints. Additionally, the joints of the limbs on the side of the newt away from the lateral camera were digitized in the dorsal view. Artificial marker points were not used in this study due to practical reasons: painted or glued-on markers simply float away when the animal is in the water. Tests in which the same sequence of images was digitized multiple times showed that the anatomic landmarks we chose could be located accurately.

To reduce digitizing error, the raw coordinates were smoothed by Gaussian filtering in Igor Pro 3.16 (WaveMetrics, Lake Oswego, OR, USA). The smoothed coordinates were then imported into Microsoft Excel (Microsoft Corp., Redmond, WA, USA), which was used to compute the angle variables defined below. For two-dimensional angles, only the coordinates from the dorsal view were used. For three-dimensional angles, the vertical coordinates from the lateral view were used as the *z*-coordinates. True three-dimensional angles were computed by Maple 6 (Maplesoft, Waterloo, Ontario, Canada). The curves produced by plotting these angle values for each sequence (the 'kinematic profile') were smoothed once more in Igor Pro; the smoothed kinematic profiles were then used for determination of minimum and maximum values for each kinematic variable (defined below).

Definition of variables

A 'stride' was defined as the time (in s) from foot contact with the ramp surface to the subsequent contact of the same foot; the left hindfoot was used as the reference in all analyses. The time during the stride in which the foot is in contact with the substrate is termed the 'stance phase' or 'duty factor', while the time that the foot is elevated and being moved into position for the start of the next stride is termed the 'swing phase'. Hildebrand-style footfall diagrams (Hildebrand, 1966, 1976) were generated by plotting duty factors as a percentage of the stride duration.

The following angles were measured in two dimensions: 'pectoral girdle angle' was defined as the angle between the line connecting the shoulder joints ('pectoral girdle line') and the direction of travel (taken as the line connecting the points on the vertebral column at the pectoral and pelvic girdles). 'Pelvic girdle angle' was defined as the angle between the line connecting the hip joints ('pelvic girdle line') and the direction of travel. 'Trunk angle' was defined as the angle between the lines connecting the point over the vertebral column midway along the trunk to the points centered over the limb girdles. 'Pectoral girdle–humerus angle' was measured between the pectoral girdle line and the line connecting the shoulder joint and the elbow. 'Pelvic girdle–femur angle' was measured between the pelvic girdle line and the line connecting the hip joint and the knee. These angles were 180° when the humerus/femur was in line with its respective girdle line, less than 180° when the humerus/femur was inclined forward of that line (protracted) and greater than 180° when inclined back of that line (retracted).

The following angles were measured in three dimensions: 'humerus–forearm angle' was measured between the line segments connecting the shoulder to elbow joint ('humerus line') and the elbow to wrist joint ('forearm line'). 'Femur–crus angle' was measured between the line segments connecting the hip to knee joint ('femur line') and the knee to ankle joint ('crus line'). Finally, 'humerus–ramp angle', 'forearm–ramp angle', 'femur–ramp angle' and 'crus–ramp angle' were defined as the angles between the appropriate limb segment lines and the ramp surface. In computing three-dimensional angles, Maple 6 is sensitive to the orientation of the line segment with respect to the reference plane. If the first point defining the line segment has a higher *z*-coordinate than the second point, the returned value is between 0° and 90°; however, if the second point has a higher *z*-coordinate than the first, the returned value is between 360° and 270°. The latter condition (second point higher than the first) often occurs in the distal limb segments, and we therefore transformed those values to center around 180° so as to facilitate comparisons with other accounts of salamander walking (e.g. Ashley-Ross, 1994a).

Several timing variables were also measured: the durations of contact of the various feet, and the relative timing between the beginning of the stride and the minima and maxima of the angular variables described above. Dividing by the stride cycle duration standardized the timing variables. Each variable is therefore expressed as a percentage of stride.

Because each stride may have differing relative proportions of stance and swing phase, the variables were further normalized by converting them into the corresponding values for a standardized stride consisting of 75% stance and 25% swing. This conversion was done following the formula described in Ashley-Ross (1995). The standardized strides were then used to generate mean kinematic profiles for the angular variables. Briefly, a custom-written macro routine in Igor Pro sorted each standardized stride into 25 bins, each accounting for 4% of the stride. The values of a given variable within each bin were averaged over all strides, and, for graphical purposes, the time (percent stride) associated with that value was taken to be the midpoint of the bin.

Statistical analysis

Direction of travel (up or down) and kinematics for the

different strides within a sequence were analyzed for statistically significant differences in StatView 5.0 for the Macintosh (SAS Institute, Cary, NC, USA) using multivariate analysis of variance (MANOVA) that considered direction, stride within sequence, and individual as the main effects. Direction and stride were treated as fixed effects, while individual was treated as a random effect. To avoid missing cells, the statistical analysis was conducted only on the strides encompassing the actual transition between media (four consecutive strides: one in which all the four limbs were out of water, one in which all the four limbs were in water, and two during which the limbs were either entering or leaving the water). Subsequent three-way analyses of variance (ANOVAs) identified individual variables that differed according to effect. Additional three-way ANOVAs tested for differences in velocity, stride length, stride duration and duty factor. In all tests, direction was tested over the direction × individual interaction term, stride was tested over the stride × individual interaction, and direction × stride was tested over the direction × stride × individual interaction. Other effects were tested over the residual. Differences were considered significant at α=0.05; due to large numbers of comparisons being made, the sequential Bonferroni method of Rice (1989) was used to establish the corrected significance level within each table.

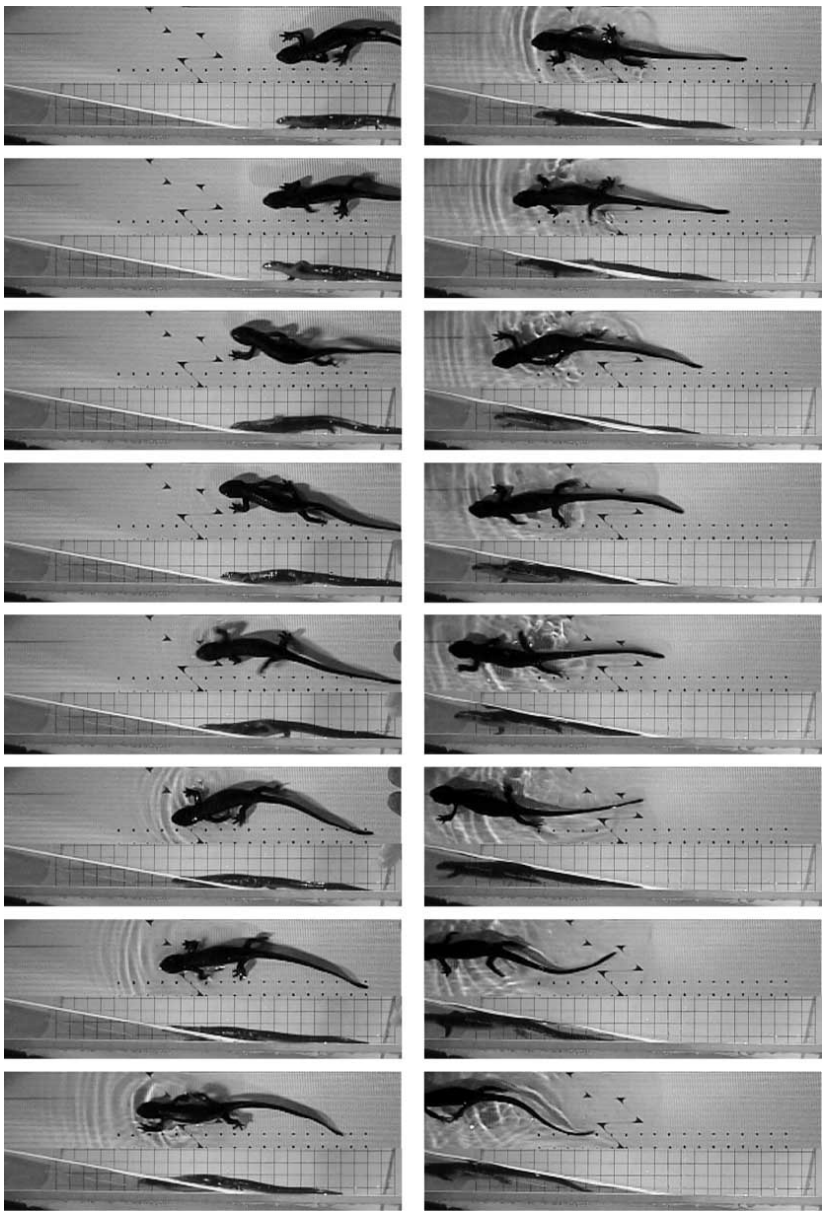

Fig. 2. Representative sequence of *Taricha* walking down a ramp into water and the transition to swimming. Panels are in sequence vertically and are each separated in time by 100 ms. In each panel, the top figure is a dorsal view, and the bottom figure is a synchronous lateral view. Both cameras were rotated to align with the ramp surface; the light-appearing diagonal line in the left half of each lateral view is the air–water interface. Note the almost complete immersion before the transition to swimming (right column). Images were cropped and composited in Adobe Photoshop 7.

Results

Gait and kinematic patterns

In sequences where the newt moved from the ramp into the water, the animal always walked into the water and continued to use the limbs for one or two strides while submerged before commencing swimming *via* lateral undulations of the trunk and tail (Fig. 2). Axial undulations began only when the newt was no longer able to make contact with the substrate using its forefeet, and typically only a single hindfoot was touching the ramp when traveling waves in the trunk and tail began. In all sequences where the newt moved from water to the ramp, the animals initially swam towards the ramp but then showed variation in the transition. In some trials, the newt switched to walking as soon as one foot touched the ramp (Fig. 3), while in others the newt continued to swim until its nose was out of the water, only then using its limbs to carry it onto the ramp. In all cases, lateral undulations of the body and tail ceased once the newt began to support its weight with its limbs. QuickTime movie files of the sequences used to construct Figs 2 and 3 may be viewed at http://www.wfu.edu/~rossma/newtmovies.html; the presence of traveling waves of undulation are more easily discerned in the movie files. Ramp-to-water (Down) sequences were characterized by strides of shorter duration and longer length than water-to-ramp (Up) sequences (Fig. 4A,B). ANOVA demonstrated a significant effect of direction on stride length ($F_{1,3}$=35.3, P=0.009), but no significant effect on duration (P=0.15). Velocity of movement was also significantly higher in Down than in Up sequences (Fig. 4C; $F_{1,3}$=388.6, P=0.003).

In both movement directions, velocity was

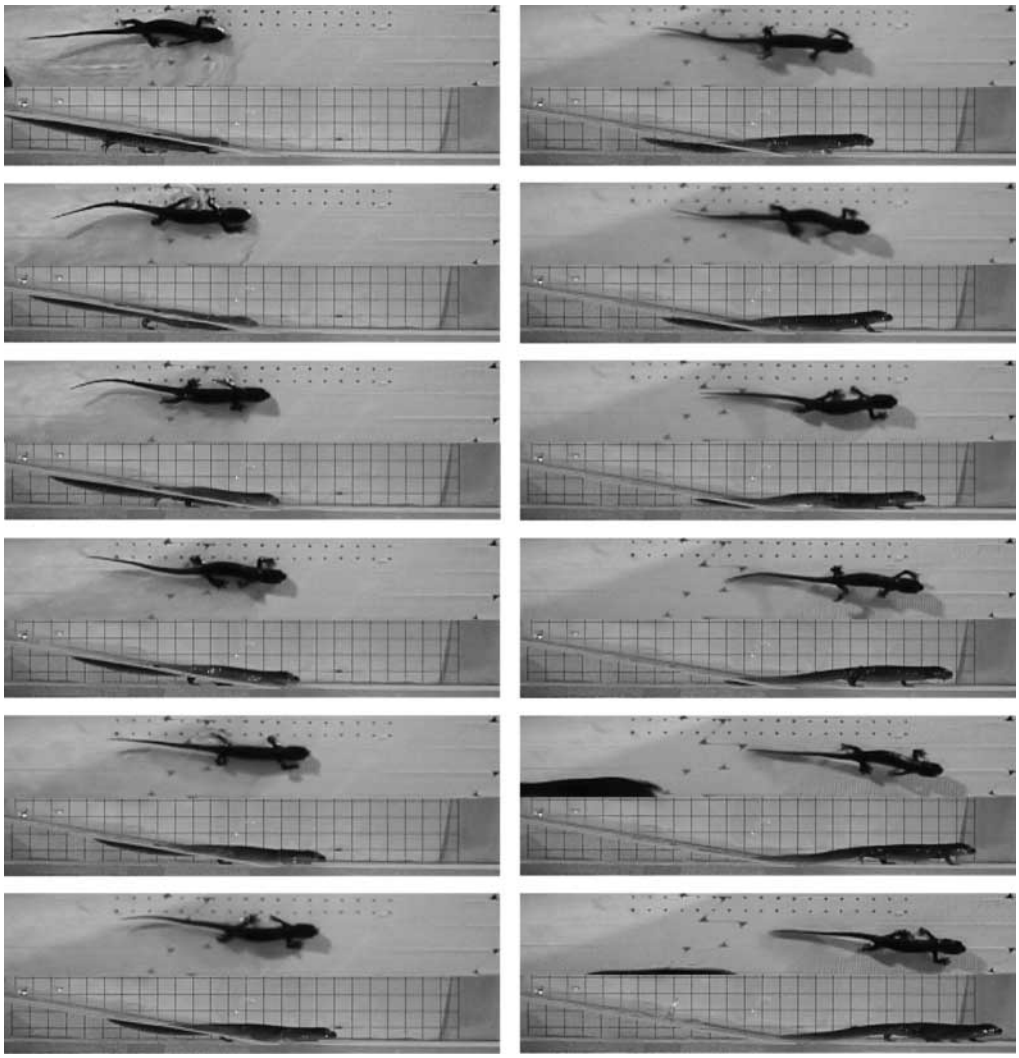

Fig. 3. Representative sequence of *Taricha* walking from water up a ramp. Panels are in sequence vertically and are each separated in time by 100 ms. In each panel, the top figure is a dorsal view, and the bottom figure is a synchronous lateral view. Both cameras were rotated to align with the ramp surface; the light-appearing diagonal line in the left half of each lateral view is the air–water interface. Note that walking commences while the newt is still submerged (left column). Images were cropped and composited in Adobe Photoshop 7.

highest in the water and declined on the ramp (Fig. 4C). This effect may be a result of the slope of the ramp. A second effect of the slope may be the increase in mean stride length with successive steps in the Down direction (Fig. 4B). By contrast, stride duration and length both declined initially in Up sequences but then remained relatively constant over most of the steps. However, none of the variables mentioned showed a significant effect of stride in the three-way ANOVA.

Average gait diagrams for Up and Down sequences are shown in Fig. 5. During terrestrial walking, *Taricha* uses a diagonal-couplets lateral sequence walk [Hildebrand, 1976; the first foot to fall after a given hindfoot is the forefoot on the same side of the body, and the footfalls of a diagonal limb pair (LH+RF, RH+LF) are closely spaced in time]. The duty factor averages 76% in fully terrestrial strides but declines with the extent of submersion to a minimum of 44% (Fig. 5; Table 1). ANOVA revealed significant effects of both stride and direction on duty factor (Table 1). In addition, the phase relationships of the limbs for Down sequences are altered in the water such that the forefoot of the diagonal limb pair falls later in the cycle. The reduction in the proportion of time the feet spend in the stance phase, coupled with the phase shift, results in a different footfall sequence underwater; newts use a gait that would be classified as a diagonal sequence walk (Fig. 5B, leftmost two strides). Finally, the stance phases of the

Table 1. *Mean (± S.D.) values for duty factor separated by direction and stride within sequence*

Effect	Direction		
Stride within sequence	Up	Down	
Ramp 3	78.5±6.8	73.7±7.4	$F_{5,14}$=7.2, P=0.002
Ramp 2	81.2±5.1	69.9±5.2	
Ramp 1	77.4±6.9	67.1±8.6	
Water 1	76.1±4.6	57.9±11.3	
Water 2	70.0±10.4	43.8±13.1	
Water 3	70.4±17.2	42.1±26.6	
	$F_{1,3}$=62.0, P=0.004		

Lines and associated F and P-values join significantly different categories.

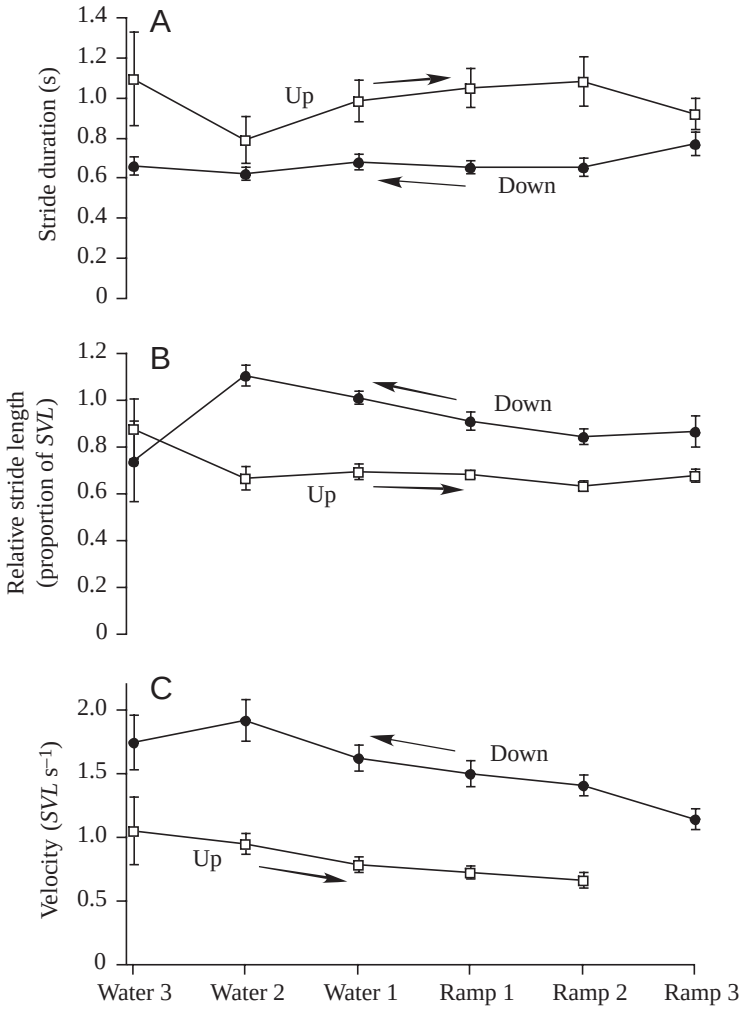

Fig. 4. Stride durations (A), relative stride lengths (B) and velocity (C) for ramp-to-water (filled circles) and water-to-ramp (open squares) sequences. Values are means ± 1 S.E.M. During the individual strides Ramp 2 and 3, the newt is completely out of water; in Water 2 and 3, the newt has all four limbs in the water. The transition between media occurs in strides Ramp 1 and Water 1. Arrows indicate the direction of locomotion.

limbs have a smaller degree of overlap when the animal is in the water, leading to periods of suspension that would be impossible for the newt when on land.

Fig. 6 shows mean kinematic profiles for the rotation of the limb girdles and overall bending of the trunk during both Down and Up sequences. In both directions of movement, the pectoral and pelvic girdle angles oscillate smoothly around 90° (perpendicular to the direction of motion) and are out of phase with each other. The trunk angle oscillates symmetrically around 180° (trunk straight). For all three variables, the angular excursions are highest when the newt is walking on the dry ramp. Angle ranges decrease, and exhibit greater variation, when the animal is submerged (Fig. 6). The reduced girdle rotation and trunk bending in water probably results from transitions to or from the use of traveling waves in the body axis.

Mean profiles for the angles between the limb girdles and the proximal limb segments are shown in Fig. 7. In both directions of movement, the pectoral girdle–humerus angle is greater than 180° for most of the strides, indicating that the humerus is retracted relative to the pectoral girdle. Humeral retraction

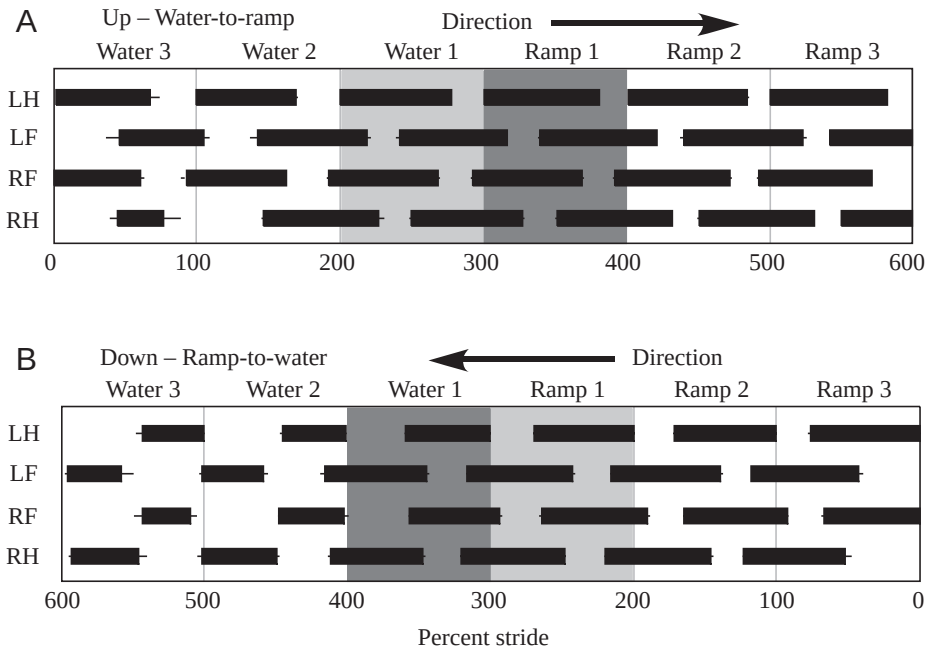

Fig. 5. Gait diagrams for transitional locomotion sequences in *Taricha*. Bars indicate periods during which the foot is on the ground. Thin bars indicate one S.E.M. of foot placement or lifting. LH, left hindfoot; LF, left forefoot; RF, right forefoot; RH, right hindfoot. (A) Water-to-ramp: transition between swimming/underwater walking and terrestrial walking. Thin gray lines separate strides. The light gray region indicates the stride during which the feet leave the water; the dark gray region indicates the stride in which all feet had left the water. Note decreasing variation in footfalls (shorter error bars) as the animal leaves the water. Mean of 20 sequences. (B) Ramp-to-water: transition between walking and swimming. Thin gray lines separate strides. The light gray region indicates the stride during which the feet enter the water; the dark gray region indicates the stride in which all feet had entered the water. For ease of comparison with Up patterns, the Down sequence has been reversed. Note increasing variation in footfalls (longer error bars) as the animal enters the water. Mean of 20 sequences. The large arrows above each panel indicate the direction of motion.

coincides with pectoral girdle rotation that advances the opposite shoulder (Figs 7, 8); thus, the forelimb appears to primarily push, rather than pull, the newt forward during the stride. Maximal retraction of the humerus reaches a sharp peak in terrestrial strides, but this peak is blunted in aquatic steps, indicating a pause before protraction of the limb commences (Fig. 7). In contrast to the humerus and pectoral girdle, the femur shows protraction relative to the pelvic girdle (angle values less than 180°). Retraction of the femur occurs in synchrony with pelvic girdle rotation that advances the opposite hip, and there is a distinct pause during terrestrial strides where the femur is held directly in line with the pelvic girdle (angle=180°; Fig. 7) before further retraction occurs. The kinematic profile of the pectoral girdle–humerus angle shows a high amount of variation during the last two strides of Down sequences, while the pelvic girdle–femur angle shows greatest variation during the first two strides of Up sequences. This pattern results from the fact that the forelimbs often do

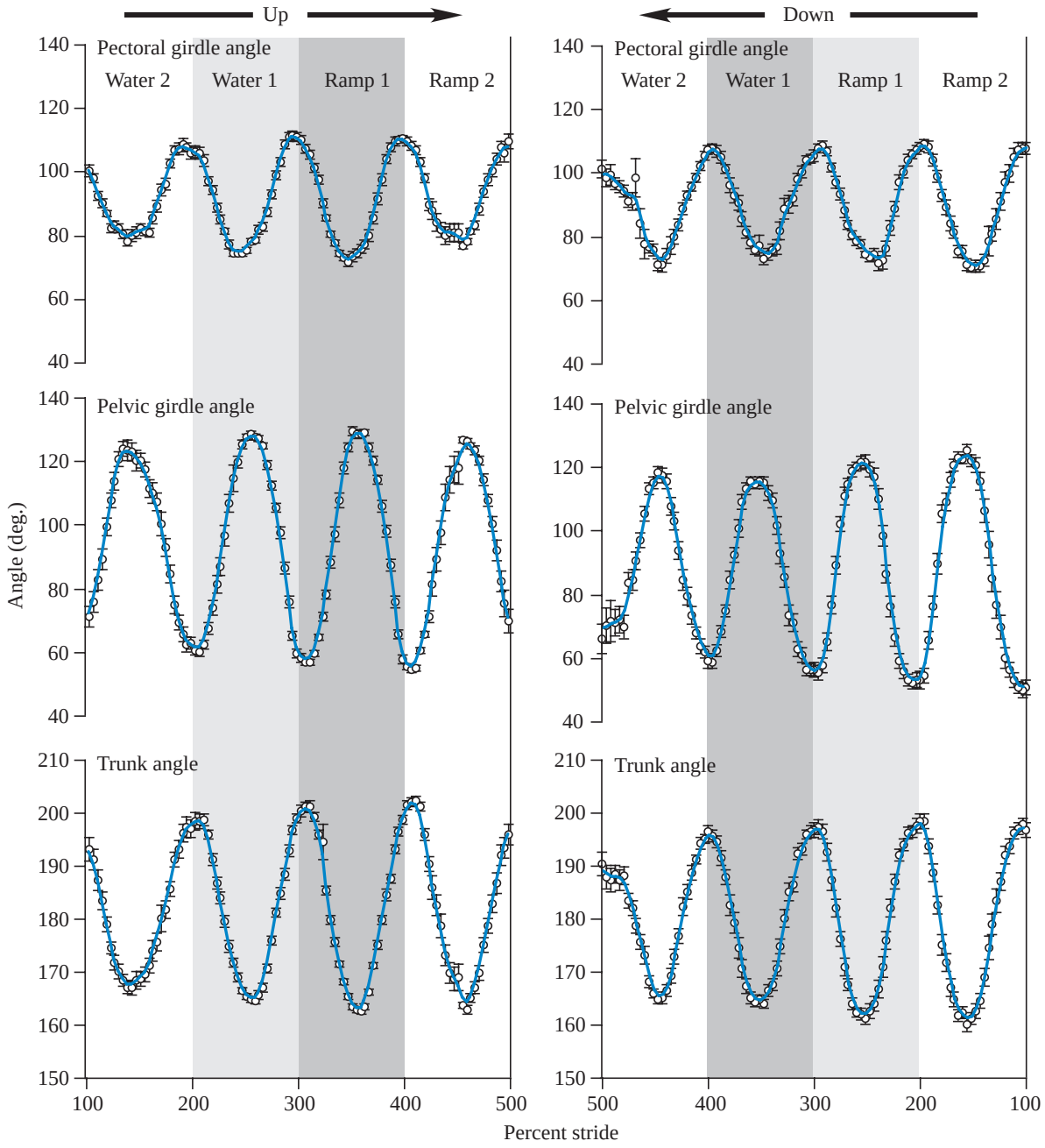

Fig. 6. Average kinematic profiles of two-dimensional pectoral girdle, pelvic girdle and overall trunk angles for Up (water-to-ramp; left panels) and Down (ramp-to-water; right panels) sequences. Symbols indicate mean values; error bars are S.E.M. The solid blue line is the smoothed average (see Materials and methods). Gray regions are as in Fig. 5. All strides begin and end with the strike of the left hindfoot. Arrows above each panel indicate the direction of motion; Down sequences have been reversed to facilitate comparison across analogous strides.

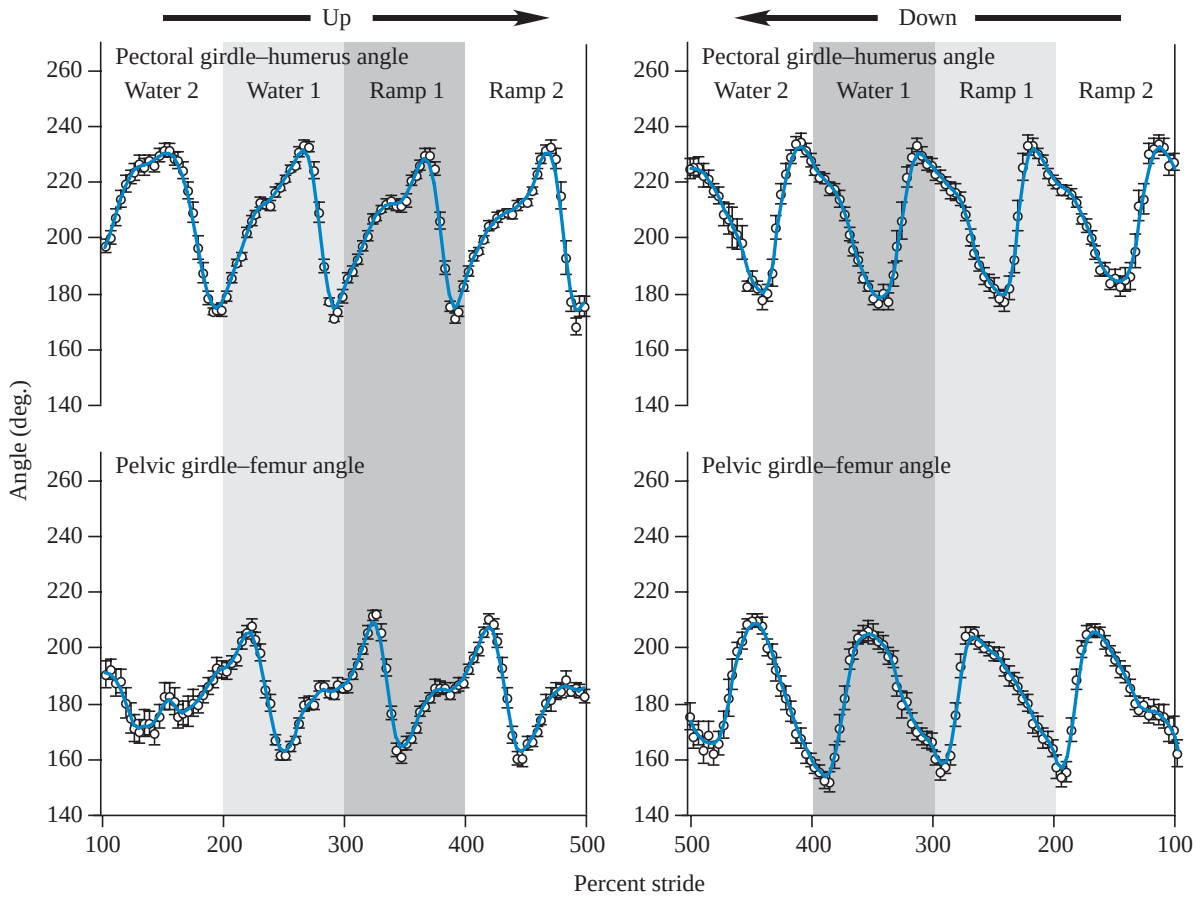

Fig. 7. Average kinematic profiles of two-dimensional angles between the pectoral girdle and humerus and between the pelvic girdle and femur for Up (water-to-ramp; left panels) and Down (ramp-to-water; right panels) sequences. Format of the figure follows the conventions of Fig. 6.

not touch the ramp during the last stride of the hindlimbs in Down sequences, while the hindlimbs often do not begin stepping motions (they are still held against the body or are being brought forward to contact the ramp) until after the first stride of the forelimbs in Up sequences.

Fig. 8 illustrates the mean kinematic profiles for the three-dimensional angles between the humerus and forearm (Fig. 8, top traces) and the femur and crus (bottom traces). For both limbs, immediately after the foot is placed on the ground the joint begins to flex and continues this motion until approximately a quarter of the way through the stride. The joint then extends until the swing phase begins, during which the joint first flexes as the limb is protracted, then extends in preparation for placement of the foot for the next stride. For both Up and Down sequences, and both fore- and hindlimbs, the joints are more extended in the water and more flexed in terrestrial locomotion.

Mean profiles for the three-dimensional angles between the limb segments (humerus, femur, forearm and crus) and the ramp surface are shown in Figs 9, 10. For the proximal limb segments, variation in their angle with the ramp is enhanced in the water, although for the majority of the time the humerus and femur are depressed from horizontal (positive angle values in Fig. 9). For distal limb segments, very little time is spent with the wrist/ankle higher than the elbow/knee (values greater than 180° in Fig. 10). During Up (but not Down) sequences, the angular excursions made by the forearm and crus are smaller and the range is displaced higher in aquatic steps than in terrestrial steps (Fig. 10), indicating that the distal limb segments are making greater angles with the substrate (perhaps as a consequence of the limbs being more extended; see above).

Multivariate comparisons

MANOVA performed on the minimum and maximum angle values and the time to minimum and maximum angles for the four strides surrounding the transition (Ramp 2, Ramp 1, Water 1 and Water 2) revealed significant differences due to direction, stride within sequence, individual and the direction × stride interaction (indicating that analogous strides in Down and Up trials were, in fact, different; Table 2).

Down and Up sequences differ in their kinematics in several respects. Tables 3 and 4 show the results of univariate ANOVAs performed on angular and timing variables. Few minimum/maximum angles proved significantly different due to direction (Table 3). The mean maximum humerus–forearm angle is larger in Down than Up sequences (Table 5), indicating that the elbow joint is more extended when *Taricha* is

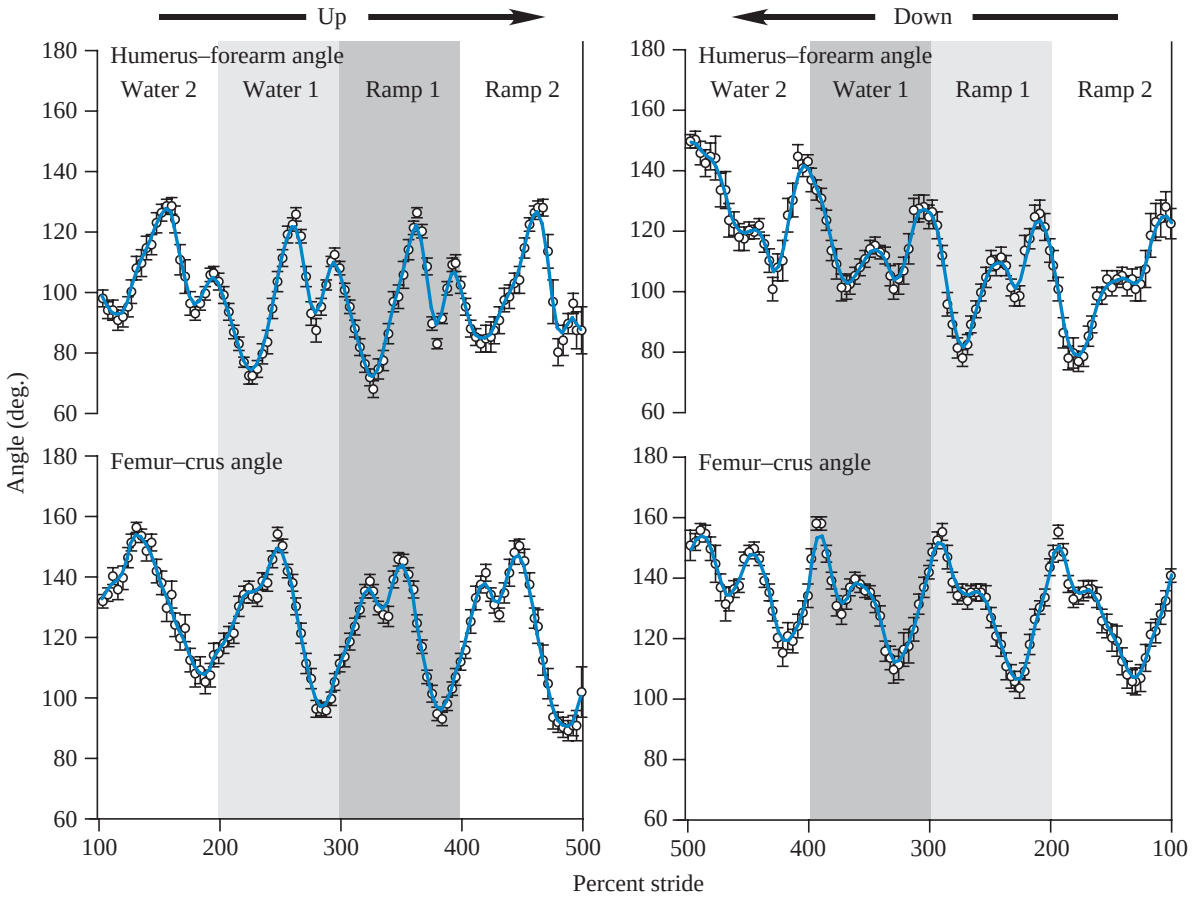

Fig. 8. Average kinematic profiles of three-dimensional angles between the humerus and forearm and between the femur and crus for Up (water-to-ramp; left panels) and Down (ramp-to-water; right panels) sequences. Format of the figure follows the conventions of Fig. 6.

Table 2. *MANOVA results for kinematic variables comparing direction of movement, stride (Ramp 2, Ramp 1, Water 1, Water 2) within sequence, and individual*

Effect	Wilks' λ	*F*	*P*
Direction (d.f.=44, 50)	0.011	100.15	<0.0001
Stride (d.f.=132, 151)	0.033	2.41	<0.0001
Individual (d.f.=132, 151)	0.002	7.64	<0.0001
Direction × stride (d.f.=132, 151)	0.020	3.07	<0.0001

descending the ramp (Fig. 8). The minimum humerus–ramp angle is less negative (indicating that the humerus is less depressed) in Up than Down trials (Table 5; Fig. 9). While not statistically significant when corrected for the number of comparisons being conducted, two additional variables showed trends towards differences due to direction (Table 3): the pectoral girdle angle range and the minimum femur–crus angle were larger in Down than Up sequences (Table 5), suggesting greater pelvic girdle rotation and less knee flexion when descending the ramp. Differences in other angular variables were not significant. The following timing variables occurred earlier in the stride in Up sequences (Figs 7–10; Table 4): minimum pelvic girdle–femur angle (protraction of the femur), minimum femur–ramp angle, minimum forearm–ramp angle, maximum crus–ramp angle and maximum femur–crus angle (Table 5). The following timing variables occurred significantly earlier in the stride in Down sequences: minimum pectoral girdle–humerus angle, maximum humerus–forearm angle, minimum femur–crus angle, minimum humerus–ramp angle, maximum forearm–ramp angle and minimum crus–ramp angle (Table 5). Three additional variables (maximum pectoral girdle–humerus angle, maximum pelvic girdle–femur angle and maximum humerus–ramp angle) approached significant differences due to direction (Table 5). Other timing variables did not differ significantly with direction (Table 4).

Significant effects of stride indicate kinematic differences due to the physical environment surrounding the newt. The minimum humerus–forearm angle is significantly increased in water (Tables 3, 6), indicating that the elbow joint is held in a more extended position. Several other angles showed differences that approached statistical significance (Table 3). The range of motion of the pelvic girdle and the trunk are greater in terrestrial strides (Fig. 6; Table 6). The maximum humerus–forearm angle is greater in the water (Fig. 8; Table 6). The humerus–ramp and femur–ramp angles show higher (less negative) values in terrestrial strides, suggesting less depression of the proximal limb segments (negative values in Fig. 9; Table 6). In the distal segments, the forearm is most

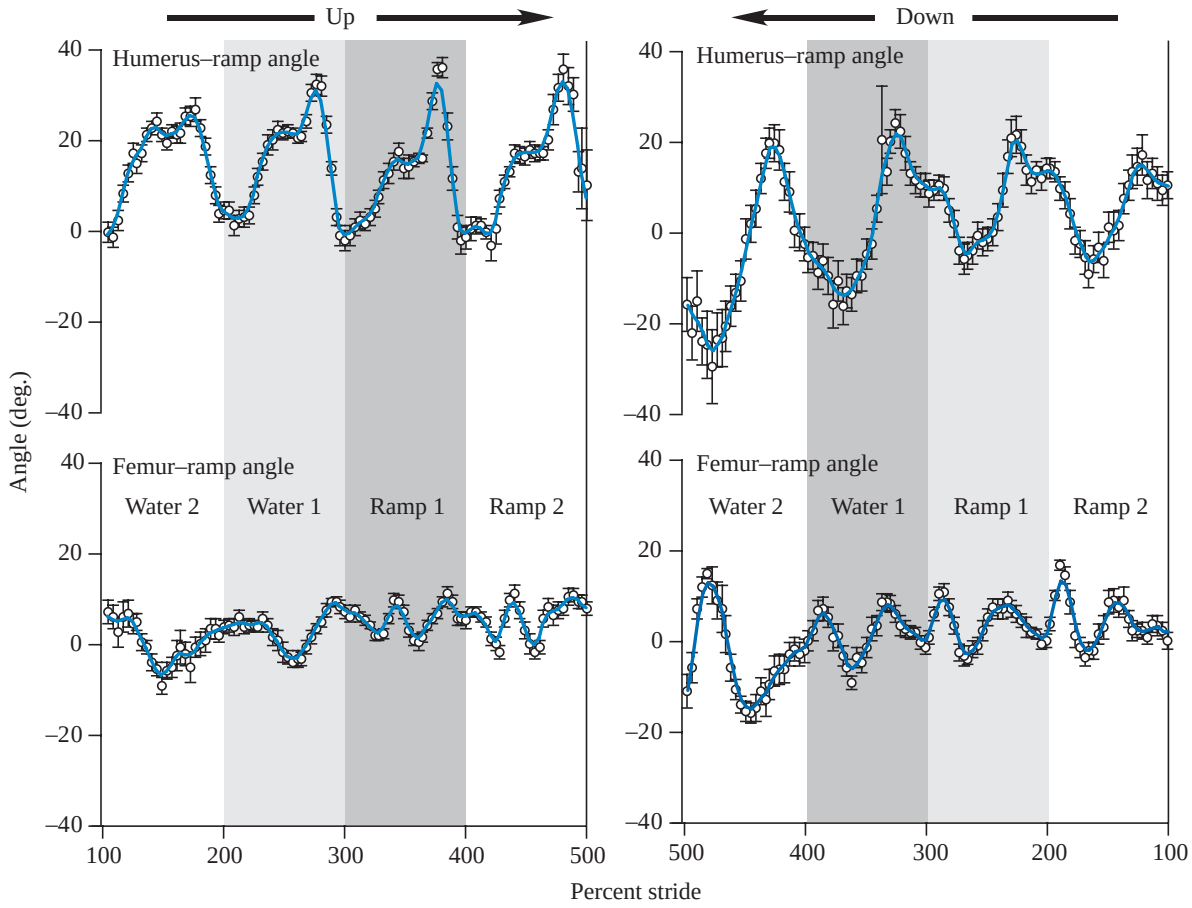

Fig. 9. Average kinematic profiles of three-dimensional angles between the humerus and ramp surface and between the femur and ramp surface for Up (water-to-ramp; left panels) and Down (ramp-to-water; right panels) sequences. Format of the figure follows the conventions of Fig. 6.

Table 3. *Individual ANOVA results for kinematic angle variables comparing direction of movement, stride (Ramp 2, Ramp 1, Water 1, Water 2) within sequence, and individual*

	Direction (d.f.=1, 3)		Stride (d.f.=3, 9)		Direction × stride (d.f.=3, 9)	
Variable (angle)	*F*	*P*	*F*	*P*	*F*	*P*
Pectoral girdle range	23.3	0.02	0.7	0.55	0.9	0.46
Pelvic girdle range	0.2	0.72	5.4	0.02	8.0	0.006
Trunk range	2.4	0.22	4.9	0.03	5.7	0.02
Min. pectoral girdle–humerus	0.8	0.44	2.3	0.14	1.6	0.25
Max. pectoral girdle–humerus	7.7	0.07	2.9	0.09	0.8	0.53
Min. pelvic girdle–femur	1.8	0.27	0.6	0.61	5.6	0.02
Max. pelvic girdle–femur	0.004	0.95	1.5	0.27	9.1	0.004
Min. humerus–forearm	5.8	0.10	12.1	**0.002**	1.3	0.34
Max. humerus–forearm	71.5	**0.003**	7.2	0.009	1.3	0.34
Min. femur–crus	21.7	0.02	4.2	0.04	5.7	0.02
Max. femur–crus	0.002	0.96	1.8	0.21	1.5	0.27
Min. humerus–ramp	72.7	**0.003**	7.1	0.009	8.9	0.004
Max. humerus–ramp	1.8	0.26	3.5	0.06	0.9	0.48
Min. forearm–ramp	2.7	0.20	6.7	0.01	1.8	0.21
Max. forearm–ramp	4.1	0.14	0.4	0.73	1.1	0.38
Min. femur–ramp	2.2	0.24	6.0	0.02	3.2	0.07
Max. femur–ramp	0.006	0.94	0.8	0.51	8.8	0.005
Min. crus–ramp	1.4	0.32	0.6	0.62	3.3	0.07
Max. crus–ramp	5.2	0.12	6.4	0.01	2.1	0.18

Bold type indicates a significant difference at α=0.05 (sequential Bonferroni-corrected).

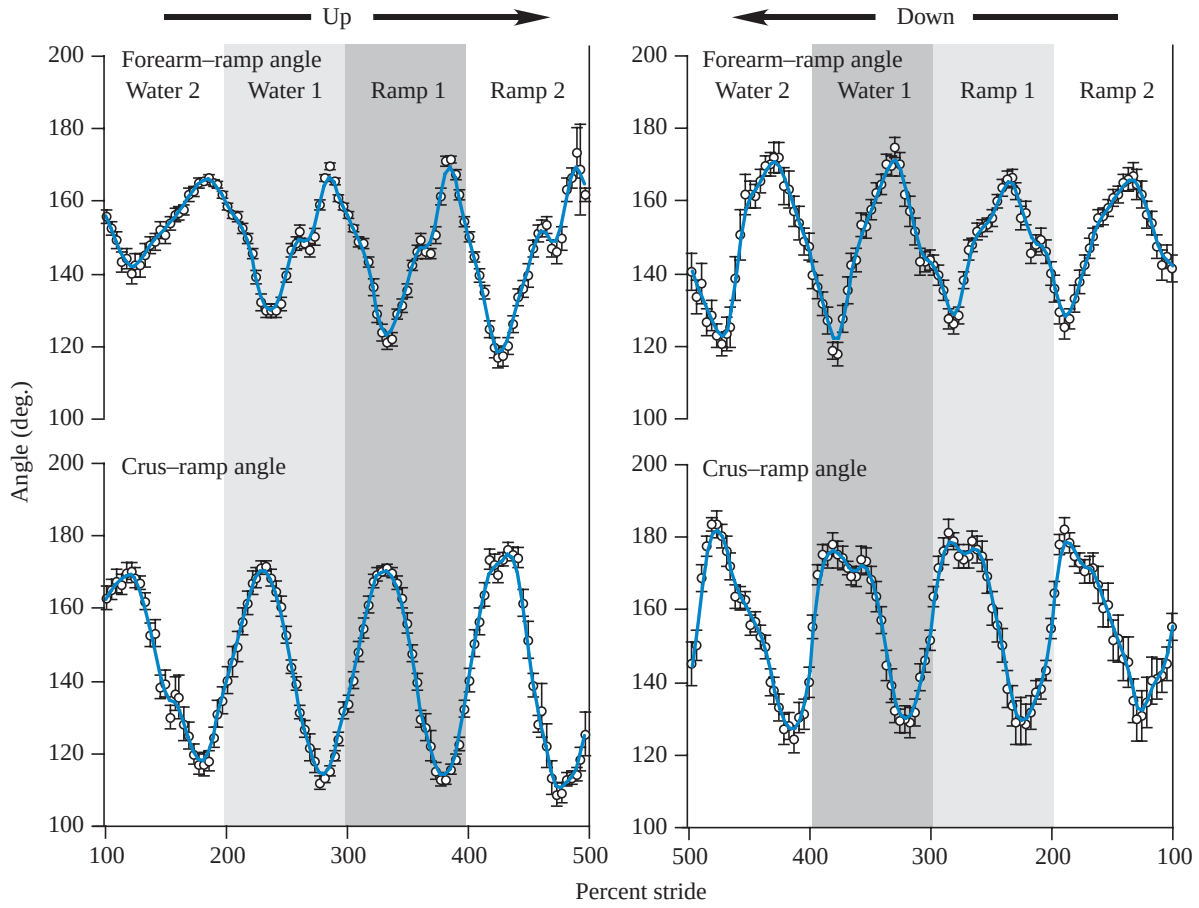

Fig. 10. Average kinematic profiles of three-dimensional angles between the forearm and ramp surface and between the crus and ramp surface for Up (water-to-ramp; left panels) and Down (ramp-to-water; right panels) sequences. Format of the figure follows the conventions of Fig. 6.

Table 4. *Individual ANOVA results for timing variables comparing direction of movement, stride (Ramp 2, Ramp 1, Water 1, Water 2) within sequence, and individual*

	Direction (d.f.=1, 3)		Stride (d.f.=3, 9)		Direction × stride (d.f.=3, 9)	
Variable (time to angle)	*F*	*P*	*F*	*P*	*F*	*P*
Max. pectoral girdle	14.4	0.03	0.09	0.97	1.9	0.19
Max. pelvic girdle	0.5	0.54	2.7	0.10	2.4	0.13
Max. trunk	0.02	0.91	9.3	**0.004**	9.4	**0.004**
Min. pectoral girdle–humerus	378.6	**0.0003**	2.1	0.17	1.4	0.30
Max. pectoral girdle–humerus	38.0	0.009	4.5	0.03	2.6	0.11
Min. pelvic girdle–femur	320.3	**0.0004**	0.7	0.58	2.0	0.18
Max. pelvic girdle–femur	34.1	0.01	32.9	**0.0001**	1.2	0.38
Min. humerus–forearm	5.1	0.11	3.2	0.08	6.3	0.01
Max. humerus–forearm	54.0	**0.005**	3.4	0.07	2.8	0.10
Min. femur–crus	65.2	**0.004**	2.4	0.13	4.6	0.03
Max. femur–crus	102.8	**0.002**	3.5	0.06	2.0	0.18
Min. humerus–ramp	158.3	**0.001**	1.4	0.30	1.7	0.23
Max. humerus–ramp	25.3	0.02	1.7	0.24	1.9	0.20
Min. forearm–ramp	128.5	**0.002**	0.8	0.54	6.7	0.01
Max. forearm–ramp	43.2	**0.007**	1.5	0.28	1.5	0.27
Min. femur–ramp	43.6	**0.007**	6.6	0.01	10.9	**0.002**
Max. femur–ramp	11.6	0.04	1.7	0.25	2.8	0.10
Min. crus–ramp	203.3	**0.0007**	0.269	0.85	1.7	0.23
Max. crus–ramp	64.2	**0.004**	1.8	0.21	3.4	0.07

Bold type indicates a significant difference at α=0.05 (sequential Bonferroni-corrected).

Table 5. *Summary of variables showing differences (according to univariate ANOVAs) due to direction*

Variable	Up	Down
Maximum humerus–forearm angle	136.7°	**150.5°**
Minimum humerus–ramp angle	**–7.7°**	–25.3°
Pectoral girdle angle range	42.7°	**50.6°**
Minimum femur–crus angle	91.2°	**100.5°**
Time to minimum pelvic girdle–femur angle	**39.6%**	94.4%
Time to minimum femur–ramp angle	**41.6%**	75.6%
Time to minimum forearm–ramp angle	**31.2%**	87.1%
Time to maximum crus–ramp angle	**27.4%**	69.8%
Time to maximum femur–crus angle	**37.3%**	73.0%
Time to minimum pectoral girdle–humerus angle	88.3%	**43.6%**
Time to maximum humerus–forearm angle	68.9%	**3.1%**
Time to minimum femur–crus angle	86.6%	**33.4%**
Time to minimum humerus–ramp angle	98.0%	**59.5%**
Time to maximum forearm–ramp angle	82.6%	**41.7%**
Time to minimum crus–ramp angle	86.6%	**33.4%**
Time to maximum pectoral girdle–humerus	56.5%	**17.6%**
Time to maximum pelvic girdle–femur	**11.6%**	60.1%
Time to maximum humerus–ramp	63.7%	**35.8%**

Bold type indicates greater values (for angular variables) or earlier occurrence in the stride (for timing variables). Variables in italic type were not statistically significant but approached significance.

Table 6. *Summary of variables showing differences (according to univariate ANOVAs) due to stride*

Variable	Water 2	Water 1	Ramp 1	Ramp 2
Min. humerus–forearm angle	**79.0°**	68.6°	63.0°	66.1°
Pelvic girdle angle range	71.4°	75.1°	79.9°	**83.3°**
Trunk angle range	37.0°	41.2°	**43.6°**	41.9°
Max. humerus–forearm angle	**150.6°**	146.2°	137.5°	140.4°
Min. humerus–ramp angle	–20.0°	–17.9°	**–12.8°**	–15.9°
Min. forearm–ramp angle	**125.7°**	111.2°	108.6°	106.4°
Min. femur–ramp angle	–21.9°	–15.3°	**–10.0°**	–12.0°
Max. crus–ramp angle	185.4°	190.3°	192.1°	**195.4°**
Time to max trunk angle	**–5.2%***	1.2%	3.8%	3.6%
Time to max pelvic girdle–femur angle	**74.2%**	84.8%	91.2%	91.3%
Time to min femur–ramp angle	**48.0%**	60.4%	65.1%	62.8%

*Negative value indicates that the event preceded the strike of the left hindfoot to begin that stride.

Bold type indicates the stride with the greatest value (for angular variables) or the earliest occurrence in the stride (for timing variables). Variables in italic type were not statistically significant but approached significance.

abducted in the water (minimum forearm–ramp angle; Fig. 10; Table 6), while the crus is most elevated on the ramp (maximum crus–ramp angle; Fig. 10; Table 6). The following timing variables occurred significantly earlier in submerged strides: time to maximum trunk angle, and maximum pelvic girdle–femur angle (Tables 4, 6). Additionally, the time to the minimum femur–ramp angle approached significance, occurring earlier in the water (Table 6). Other timing variables showed no significant effect of stride (Table 4).

Few variables demonstrated significant direction × stride effects (Tables 3, 4); in those cases, examination of mean values showed that the Water 2 stride usually exhibited the anomalous pattern leading to the significant interaction (data not shown). A significant effect of individual was found for most angular variables but few timing variables (data not shown).

Discussion

Effect of incline on kinematics

A confounding factor in the attempt to determine kinematic differences between terrestrial and aquatic strides is the necessity for an inclined ramp on which to test the newts. Locomotion on an incline has been shown to alter energetics, footfall patterns and muscle activity in a variety of taxa (Pierotti et al., 1989; Full and Tullis, 1990; Vilensky et al., 1994; Farley and Emshwiller, 1996; Farley, 1997; Carlson-Kuhta et al., 1998; Irschick and Jayne, 1998; Biewener and Gillis, 1999; Hoyt et al., 2000; Swanson and Caldwell, 2000; Wickler et al., 2000; Gillis and Biewener, 2002). While kinematic studies have concentrated primarily on the effects of ascending a slope (Carlson-Kuhta et al., 1998; Irschick and Jayne, 1998; Hoyt et al., 2000, 2002), significant effects on limb movement patterns have also been demonstrated for descending slopes (Jayne and Irschick, 1999).

During terrestrial strides, uphill and downhill sequences showed differences in the stride length and duration (Fig. 4A,B) and velocity of movement (Fig. 4C). Uphill strides were characterized by greater stride durations, shorter stride lengths and slower speeds, similar to previous results (Farley, 1997; Irschick and Jayne, 1998; Hoyt et al., 2000). Duty factors were lower in downhill strides (Table 1), although the values in both directions are similar to those reported for other salamanders during level terrestrial walking (Ashley-Ross, 1994a; Fig. 5). In the current study, velocities of downhill strides were significantly higher than uphill strides (see Results); it is likely that the reduced duty factors in Down strides result at least partially from the increased speed, as has been reported in earlier work (Ashley-Ross, 1994b).

In other vertebrates, the kinematics of uphill locomotion are characterized by increased flexion of the limbs (particularly the knee joint) early in the stance, greater extension of knee and ankle joints at the end of stance, and increased femoral retraction (Vilensky et al., 1994; Carlson-Kuhta et al., 1998; Jayne and Irschick, 1999). Downhill locomotion shows greater extension of the limbs and greater femoral protraction (Jayne and Irschick, 1999). *Taricha* follows the pattern seen for other vertebrates in the relative amount of limb (elbow and knee joint) extension (Fig. 8; Table 5). Greater limb extension may be a result of the higher velocities of downhill strides; however, joint angles have been shown not to change significantly with speed in salamanders (Ashley-Ross, 1994b). Contrary to results from lizards, *Taricha* demonstrates no significant differences in the extent of humerus/femur protraction and retraction. It is

possible that the angle of inclination used in the present study (15°) was too small to induce the newts to alter the extent of limb protraction and retraction [Jayne and Irschick (1999) used an angle of 30° for uphill and downhill trials].

Effect of environment on kinematics

Examination of the average gait diagrams in Fig. 5 reveals a striking difference between terrestrial and submerged strides: the duty factor declines significantly (Table 1) with the degree of immersion of the newt. While the pattern is true for both directions, it is particularly evident for Down sequences; for terrestrial strides, each foot is in contact with the ground for approximately three-quarters of the stride duration, while for submerged strides, the period of foot contact declines to less than half of the stride (Fig. 5B). Furthermore, as the newt walks underwater, the strike of each forefoot is delayed relative to the diagonal hindfoot. The end result of the reduced duty factor and the phase shift in the footfalls is a change in gait to a diagonal sequence walk (Fig. 5B, leftmost two strides; Hildebrand, 1976). *Taricha* walking underwater on a level surface also shows the diagonal sequence pattern (M.A.A.-R., unpublished data). This footfall pattern is never seen in salamanders walking on land (Ashley-Ross, 1994a). Finally, an additional novelty of underwater walking is that the buoyant support of the water makes it possible for newts, with a sprawled posture, to reduce the period of limb support to such an extent that there are periods of suspension during the stride, as is seen in anglerfishes (Edwards, 1989) and crabs (Martinez et al., 1998).

The MANOVA revealed several kinematic differences between strides on land and in the water, distinct from differences due to the direction of movement (uphill or downhill). Smaller ranges of motion in the pelvic girdle and trunk in submerged strides (Fig. 6) may be related to the incipient shift from standing to traveling waves in the trunk as the animal transitions to swimming. The greater extension the elbow joint shows in the water (Fig. 8; Tables 3, 6) is similar to results in turtles when swimming and walking kinematics are compared (Gillis and Blob, 2001) although, since the turtles were swimming rather than walking underwater, such a conclusion must be made with caution. In swimming, a more-extended limb can function as an improved paddle; however, since the newts were walking underwater, this is unlikely to have been a goal of the observed limb posture.

Buoyancy when submerged is likely to have made possible the greater adduction of the proximal limb segments (Fig. 9) and the more flattened angles of the distal segments (Fig. 10). By contrast, the requirements of supporting all of the body weight on the limbs when moving out of the water necessitates the more acute angles of the distal segments (both to orient the bones to take a greater proportion of the load in compression and to raise the body off the ramp surface). The few changes in timing variables from terrestrial to underwater strides suggest that the basic pattern of movement functions well in either environment, and only small alterations in the timing of lateral flexion and the beginning of hindlimb protraction (time to maximum pelvic girdle–femur angle) are necessary. Further studies to quantify the use of the limbs while walking underwater on a level substrate are underway; comparison with transitional locomotion should clarify environmental effects on walking kinematics.

Implications for the neural control of swimming/walking transitions

Most walking salamanders typically generate standing waves in the trunk, resulting in increased stride length (Daan and Belterman, 1968; Frolich and Biewener, 1992; Carrier, 1993; Ashley-Ross, 1994a), although some elongate forms use traveling waves during terrestrial locomotion, particularly at increased speed (Daan and Belterman, 1968). By contrast, swimming salamanders generate a pattern of traveling waves in the body axis, which function to propel the animal (Frolich and Biewener, 1992; Gillis, 1997) by anguilliform locomotion, with no participation by the limbs.

Neural networks that successfully model the swimming and terrestrial (trotting) gaits of a salamander also show a separation between locomotion *via* traveling waves and standing waves/limbs (Ijspeert, 2000, 2001). In the model, tonic input to the central pattern generator (CPG) for the body axis alone produces traveling waves, while tonic stimulation applied to both the axial and limb CPGs results in standing waves plus limb oscillations (Ijspeert, 2001).

Our results lend support to the separation of swimming and walking patterns. In no case did we observe traveling waves in the body axis coupled with limb movements. However, the aquatic locomotor repertoire of the newt is by no means limited to only swimming; *Taricha* always walked into the water until fully submerged and is capable of walking underwater. Analysis of the sequence of strides in the ramp-to-water trials showed that there was a smooth, though well-defined, transition between walking and swimming (Fig. 2). Due to the support of the water, the forelimbs would typically lose contact with the ramp surface after two or three underwater strides. At this point, the hindlimbs would go through one more cycle of protraction/retraction, and the transition to traveling waves would always occur after a final push-off from the second hindlimb (see QuickTime movies referenced above). The coordination of the final hindlimb retraction with the beginning of traveling waves argues that the CPGs responsible for the swimming and walking patterns are not totally separate and may be capable of more extensive interaction than previously thought.

We have recorded kinematic patterns for the transitions between swimming and walking; the observed movements may be strongly influenced by the medium surrounding the newt and not necessarily accurate reflections of the motor output of the nervous system. Further research is needed to document the activity patterns of axial and limb muscles during transitional locomotion in order to understand the interaction between the two propulsive systems.

We thank Brad Chadwell and two anonymous reviewers for helpful comments on the manuscript. Supported by a National Science Foundation grant (IBN 0316331) to M.A.A.-R.

References

Ashley-Ross, M. A. (1994a). Hind limb kinematics during terrestrial locomotion in a salamander (*Dicamptodon tenebrosus*). *J. Exp. Biol.* **193**, 255-283.

Ashley-Ross, M. A. (1994b). Metamorphic and speed effects on hind limb kinematics during terrestrial locomotion in the salamander *Dicamptodon tenebrosus*. *J. Exp. Biol.* **193**, 285-305.

Ashley-Ross, M. A. (1995). Patterns of hind limb motor output during walking in the salamander *Dicamptodon tenebrosus*, with comparisons to other tetrapods. *J. Comp. Physiol. A* **177**, 273-285.

Barclay, O. R. (1946). The mechanics of amphibian locomotion. *J. Exp. Biol.* **23**, 177-203.

Biewener, A. A. and Corning, W. R. (2001). Dynamics of mallard *(Anas platyrynchos)* gastrocnemius function during swimming versus terrestrial locomotion. *J. Exp. Biol.* **204**, 1745-1756.

Biewener, A. A. and Gillis, G. B. (1999). Dynamics of muscle function during locomotion: accommodating variable conditions. *J. Exp. Biol.* **202**, 3387-3396.

Campbell, N. A., Reece, J. B. and Mitchell, L. G. (1999). *Biology*. 5th edition. Menlo Park, CA: Benjamin/Cummings.

Carlson-Kuhta, P., Trank, T. V. and Smith, J. L. (1998). Forms of forward quadrupedal locomotion. II. A comparison of posture, hindlimb kinematics, and motor patterns for upslope and level walking. *J. Neurophysiol.* **79**, 1687-1701.

Carrier, D. R. (1993). Action of the hypaxial muscles during walking and swimming in the salamander *Dicamptodon ensatus*. *J. Exp. Biol.* **180**, 75-83.

Clack, J. A. (2002a). An early tetrapod from "Romer's Gap". *Nature* **418**, 72-76.

Clack, J. A. (2002b). *Gaining Ground: the Origin and Evolution of Tetrapods.* Bloomington, IN: Indiana University Press.

Coates, M. I. and Clack, J. A. (1991). Fish-like gills and breathing in the earliest known tetrapod. *Nature* **352**, 234-236.

Daan, S. and Belterman, T. (1968). Lateral bending in the locomotion of some lower tetrapods. *Proc. Ned. Akad. Wetten.* **C71**, 245-266.

Duellman, W. E. and Trueb, L. (1986). *Biology of Amphibians*. New York: McGraw-Hill.

Edwards, J. L. (1977). The evolution of terrestrial locomotion. In *Major Patterns in Vertebrate Evolution* (ed. M. K. Hecht, P. C. Goody and B. M. Hecht), pp. 553-576. New York: Plenum.

Edwards, J. L. (1989). Two perspectives on the evolution of the tetrapod limb. *Am. Zool.* **29**, 235-254.

Ellerby, D. J., Spierts, I. L. Y. and Altringham, J. D. (2001). Fast muscle function in the European eel (*Anguilla anguilla* L.) during aquatic and terrestrial locomotion. *J. Exp. Biol.* **204**, 2231-2238.

Farley, C. T. (1997). Maximum speed and mechanical power output in lizards. *J. Exp. Biol.* **200**, 2189-2195.

Farley, C. T. and Emshwiller, M. (1996). Efficiency of uphill locomotion in nocturnal and diurnal lizards. *J. Exp. Biol.* **199**, 587-592.

Fricke, H., Reinicke, O., Hofer, H. and Nachtigall, W. (1987). Locomotion of the coelacanth *Latimeria chalumnae* in its natural environment. *Nature* **329**, 331-333.

Frolich, L. M. and Biewener, A. A. (1992). Kinematic and electromyographic analysis of the functional role of the body axis during terrestrial and aquatic locomotion in the salamander *Ambystoma tigrinum*. *J. Exp. Biol.* **162**, 107-130.

Full, R. J. and Tullis, A. (1990). Energetics of ascent: insects on inclines. *J. Exp. Biol.* **149**, 307-317.

Gao, K.-Q. and Shubin, N. H. (2001). Late Jurassic salamanders from northern China. *Nature* **410**, 574-577.

Gillis, G. B. (1997). Anguilliform locomotion in an elongate salamander (*Siren intermedia*): effects of speed on axial undulatory movements. *J. Exp. Biol.* **200**, 767-784.

Gillis, G. B. (1998a). Environmental effects on undulatory locomotion in the American eel *Anguilla rostrata*: kinematics in water and on land. *J. Exp. Biol.* **20**, 949-961.

Gillis, G. B. (1998b). Neuromuscular control of anguilliform locomotion: patterns of red and white muscle activity during swimming in the American eel *Anguilla rostrata*. *J. Exp. Biol.* **201**, 3245-3256.

Gillis, G. B. (2000). Patterns of white muscle activity during terrestrial locomotion in the American eel *(Anguilla rostrata). J. Exp. Biol.* **203**, 471-480.

Gillis, G. B. and Biewener, A. A. (2000). Hindlimb extensor muscle function during jumping and swimming in the toad *(Bufo marinus). J. Exp. Biol.* **203**, 3547-3563.

Gillis, G. B. and Biewener, A. A. (2002). Effects of surface grade on proximal hindlimb muscle strain and activation during rat locomotion. *J. Appl. Physiol.* **93**, 1731-1743.

Gillis, G. B. and Blob, R. W. (2001). How muscles accommodate movement in different physical environments: aquatic vs. terrestrial locomotion in vertebrates. *Comp. Biochem. Physiol. A* **131**, 61-75.

Hammond, L., Altringham, J. D. and Wardle, C. S. (1998). Myotomal slow muscle function of rainbow trout *Oncorhynchus mykiss* during steady swimming. *J. Exp. Biol.* **201**, 1659-1671.

Hildebrand, M. (1966). Analysis of the symmetrical gaits of tetrapods. *Fol. Biotheor.* **6**, 9-22.

Hildebrand, M. (1976). Analysis of tetrapod gaits: general considerations and symmetrical gaits. In *Neural Control of Locomotion* (ed. R. M. Herman, S. Grillner, P. S. G. Stein and D. G. Stuart), pp. 203-236. New York: Plenum Press.

Hildebrand, M. (1985). Walking and running. In *Functional Vertebrate Morphology* (ed. M. Hildebrand, D. Bramble, K. F. Liem and D. Wake), pp. 38-57. Cambridge, MA: Belknap Press of Harvard University Press.

Hoyt, D. F., Molinari, M., Wickler, S. J. and Cogger, E. A. (2002). Effect of trotting speed, load and incline on hindlimb stance-phase kinematics. *Equine Vet. J.* **Suppl. 34**, 330-336.

Hoyt, D. F., Wickler, S. J. and Cogger, E. A. (2000). Time of contact and step length: the effect of limb length, running speed, load carrying and incline. *J. Exp. Biol.* **203**, 221-227.

Ijspeert, A. J. (2000). A 3-D biomechanical model of the salamander. *Proc. 2nd Intl. Conf. Virtual Worlds* (ed. J.-C. Heudin), pp. 225-234. Heidelberg, Germany: Springer-Verlag.

Ijspeert, A. J. (2001). A connectionist central pattern generator for the aquatic and terrestrial gaits of a simulated salamander. *Biol. Cyber.* **84**, 331-348.

Irschick, D. J. and Jayne, B. C. (1998). Effects of incline on speed, acceleration, body posture and hindlimb kinematics in two species of lizard *Callisaurus draconoides* and *Uma scoparia. J. Exp. Biol.* **201**, 273-287.

Jayne, B. C. and Irschick, D. J. (1999). Effects of incline and speed on the three-dimensional hindlimb kinematics of a generalized iguanian lizard *(Dipsosaurus dorsalis). J. Exp. Biol.* **202**, 143-159.

Jayne, B. C. and Lauder, G. V. (1994). How swimming fish use slow and fast muscle fibers: implications for models of vertebrate muscle recruitment. *J. Comp. Physiol. A* **175**, 123-131.

Jayne, B. C. and Lauder, G. V. (1995). Red muscle motor patterns during steady swimming in largemouth bass: effects of speed and correlations with axial kinematics. *J. Exp. Biol.* **198**, 1575-1587.

Long, J. H., Jr, Hale, M. E., McHenry, M. J. and Westneat, M. W. (1996). Functions of fish skin: the mechanics of steady swimming in longnose gar *Lepisosteus osseus*. *J. Exp. Biol.* **199**, 2139-2151.

Martinez, M. M., Full, R. J. and Koehl, M. A. (1998). Underwater punting by an intertidal crab: a novel gait revealed by the kinematics of pedestrian locomotion in air versus water. *J. Exp. Biol.* **201**, 2609-2623.

Pace, C. M., Blob, R. W. and Westneat, M. W. (2001). Comparative kinematics of the forelimb during swimming in red-eared slider *(Trachemys scripta)* and spiny softshell *(Apalone spinifera)* turtles. *J. Exp. Biol.* **204**, 3261-3271.

Petranka, J. W. (1998). *Salamanders of the United States and Canada.* Washington, DC: Smithsonian Institution Press.

Pierotti, D. J., Roy, R. R., Gregor, R. J. and Edgerton, V. R. (1989). Electromyographic activity of cat hindlimb flexors and extensors during locomotion at varying speeds and inclines. *Brain Res.* **27**, 57-66.

Pough, F. H., Janis, C. M. and Heiser, J. B. (2002). *Vertebrate Life.* 6th edition. Upper Saddle River, NJ: Prentice Hall.

Rice, W. R. (1989). Analyzing tables of statistical tests. *Evolution* **43**, 223-225.

Swanson, S. C. and Caldwell, G. E. (2000). An integrated biomechanical analysis of high speed incline and level treadmill running. *Med. Sci. Sports Exerc.* **32**, 1146-1155.

Vilensky, J. A., Moore, A. M. and Libii, J. N. (1994). Squirrel monkey locomotion on an inclined treadmill: implications for the evolution of gaits. *J. Human Evol.* **26**, 375-386.

Wickler, S. J., Hoyt, D. F., Cogger, E. A. and Hirschbein, M. H. (2000). Preferred speed and cost of transport: the effect of incline. *J. Exp. Biol.* **203**, 2195-2200.